# Inverse Melting in Syndiotactic Polystyrene

**Catharina S. J. van Hooy-Corstjens,[†,‡] Günther W. H. Höhne,[†] and Sanjay Rastogi*[,†]**

*Dutch Polymer Institute / Department of Chemical Engineering, Eindhoven University of Technology, P.O. Box 513, 5600 MB Eindhoven, The Netherlands, and Centre for Biomaterials Research, University of Maastricht, P.O. Box 616, 6200 MD Maastricht, The Netherlands*

*Received September 3, 2004; Revised Manuscript Received November 24, 2004*

ABSTRACT: Syndiotactic polystyrene (sPS) is a semicrystalline polymer for which several crystalline structures can be obtained. Cold crystallization of an amorphous sPS sample results in the formation of the α-phase, for which a close packing of the chains is hindered by the phenyl rings. This results in the unusual situation that the density of the crystalline phase (1.03 g cm$^{-3}$) is lower than that of amorphous sPS (1.04 g cm$^{-3}$). It is shown that as a result a line where the difference in specific volume between the liquid and crystal is zero ($\Delta V = 0$ line) is observed in the $p-T$ phase diagram (similar to P4MP1). At the point where this line intersects with the melting line the slope of the melting line becomes negative. Another remarkable phenomenon is that the crystalline α-phase disorders either with the application of pressure at room temperature (below $T_g$) or on cooling isobarically at high pressure. These observations, obtained via WAXD, SAXS, HP-DSC, and Raman spectroscopy experiments, give an indication for the existence of a reentrant phase behavior, first described by Tamman in 1903.

## 1. Introduction

Syndiotactic polystyrene (sPS) is a polymorphic material, for which several crystalline modifications, with chains in either a planar zigzag or helical conformation, can be obtained. About two decades ago, Ishihara et al. were the first to synthesize this stereoregular form of polystyrene using a single-site metallocene catalyst, consisting of titanium compounds with methylaluminoxane.[1] Depending on the crystallization conditions, four main crystalline structures, designated as α, *β*, *γ*, and *δ*, can be distinguished.[2−4] The *γ*- and *δ*-phase contain chains with a $t_2g_2$ conformation, resulting in a helical symmetry. In the primary crystalline polymorphs, the α- and *β*-phase, the backbone of the polymer chain adopts an all-trans planar zigzag ($t_4$) conformation, with an identity unit of 5.1 Å.[4] The *β*-phase, formed during crystallization on cooling from the melt, is characterized by an orthorhombic packing of the chains with a theoretical density of 1.09 g cm$^{-3}$.[5,6] On the other hand, for the α-phase, which is obtained by cold crystallization from the amorphous phase, a close packing of chains is hindered by the phenyl rings, resulting in a hexagonal structure.[7] Because of the loose packing of chains, this phase has a theoretical density of only 1.03 g cm$^{-3}$, which is reported to be even lower than that of amorphous sPS (1.04 g cm$^{-3}$).[7,8] Barnes et al. have shown that as a result of the close resemblance of the density of the amorphous and the crystalline phase, the small-angle X-ray scattering pattern hardly shows any contrast below $T_g$.[9]

So far, such an inverse density relationship between the crystal and amorphous phases ($\rho_c < \rho_a$) is observed for two other polymers, i.e., isotactic poly(4-methylpentene-1) (P4MP1)[10−14] and form III of syndiotactic poly(*p*-methylstyrene) (s-PPMS).[15] This unusual density relationship gives rise to remarkable phenomena. For P4MP1 it has been shown that at room temperature (below $T_g$) the initially crystalline material disorders with the application of pressure, the process being reversible. Moreover, the application of pressure at a temperature just below the atmospheric fusion temperature results in melting of the crystalline phase, while on releasing pressure isothermally the crystalline phase is recovered. The latter suggests the existence of a negative slope of the $T_m$ line with increasing pressure. This means that an inversion of the Clapeyron equation (eq 1) occurs for P4MP1

$$\frac{dT_m}{dp} = \frac{\Delta V_f}{\Delta S_f} = T_m \frac{\Delta V_f}{\Delta H_f} \tag{1}$$

with $\Delta V_f$, $\Delta S_f$, and $\Delta H_f$ the volume, entropy, and enthalpy of fusion, respectively.

At high pressures, melting results in a decrease of volume ($\Delta V_f < 0$), while both the enthalpy ($\Delta H_f > 0$) and the entropy ($\Delta S_f > 0$) of the system increase. Similar effects as for P4MP1 have been observed for form III of s-PPMS.[15]

Rastogi et al.[12] state that the interesting phenomena in the $p-T$ diagram of P4MP1, like an inversion in the Clapeyron equation and disordering below $T_g$ with the application of pressure, might provide experimental prove for the universal pressure−temperature phase diagram as proposed by Gustav Tamman in 1903.[16] This diagram shows a reentrant phase behavior, as given in Figure 1. The origin of such reentrant phase behavior is contributed to the existence of a line where the specific volumes of the liquid and the crystal are equal ($\Delta V = 0$) and another line where the enthalpy of the liquid and crystal are equal ($\Delta H = 0$). When the $\Delta V = 0$ line intersects with the melting line, the situation arises where $\Delta V_f = 0$, and from eq 1 it follows that at this point $dT_m/dp = 0$. At higher pressures $dT_m/dp$ will become negative (region II in the phase diagram), implying that the slope of the melting line in the $p-T$ diagram inverts and becomes negative. With further increase of pressure, a situation arises where $\Delta H_f$ becomes zero, and at this point, $dT_m/dp$ will become

[†] Dutch Polymer Institute/Department of Chemical Engineering, Eindhoven University of Technology.
[‡] Centre for Biomaterials Research, University of Maastricht.

10.1021/ma048190b CCC: $30.25 
Published on Web 02/03/2005

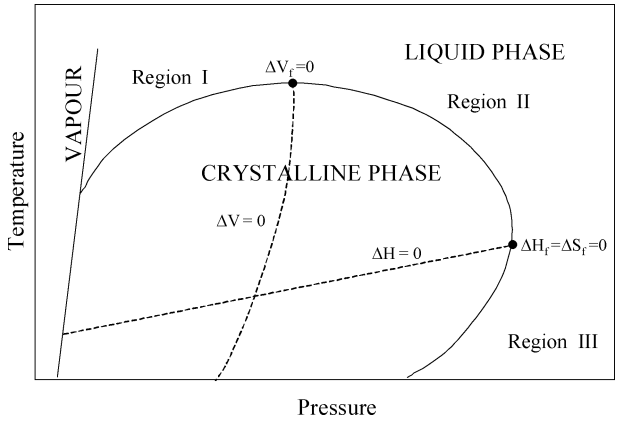


**Figure 1.** Universal pressure−temperature phase diagram as proposed by Tamman.[16] Region I: $\Delta V_f > 0$, $\Delta H_f > 0$, $\Delta S_f > 0$. Region II: $\Delta V_f < 0$, $\Delta H_f > 0$, $\Delta S_f > 0$. Region III: $\Delta V_f < 0$, $\Delta H_f < 0$, $\Delta S_f < 0$.

infinite. At lower temperatures, within region III of the phase diagram, the melting should then be reversed.

It is to be noted that within region I and II $\Delta H_f$ is positive, suggesting that the crystal to liquid transformation is endothermic in nature. In region III, on the other hand, $\Delta H_f$ becomes negative, implying that within this region the crystal to liquid (or amorphous) phase should be an exothermic process.

Experimental evidence for the existence of the three different regions has been obtained recently for P4MP1. The existence of the $\Delta V = 0$ line in the phase diagram of P4MP1 was realized by small-angle X-ray scattering experiments performed by van Ruth et al.,[17] whereas the inversion in $\Delta H$ in P4MP1 was shown by HP-DSC experiments.[12,13]

On the basis of its anomalous density relationship, a similar behavior may be observed for the crystalline α-phase of sPS. In this article, the results on isothermal pressure experiments and isobaric heating experiments will be described. The data are obtained via in-situ wide-angle X-ray diffraction (WAXD), small-angle X-ray scattering (SAXS), high-pressure differential scanning calorimetry (HP-DSC), and Raman spectroscopy.

## 2. Materials and Methods

For all experiments a commercial sPS grade from Dow Chemical, Terneuzen (NL), with a molar mass of 400 kg mol$^{-1}$, was used. Thin plates (1−4 mm thick, depending on the experimental method) containing the crystalline α-phase were prepared by annealing amorphous material at 190 °C for about 15−20 h. The amorphous material was obtained by quenching the melt in an ice bath. After the annealing procedure a conventional DSC run showed a glass transition at 96 °C with a $\Delta c_p$ of 0.16 and a (double) melting peak between 260 and 270 °C with a heat of fusion of 25 J g$^{-1}$, resulting in a degree of amorphous $x_a = 0.55$ and a degree of crystallinity $x_c = 0.24$, respectively. The remaining fraction (0.21) is attributed to the rigid amorphous fraction.

To study the influence of pressure on the different modifications of sPS, a piston−cylinder type of pressure cell was used.[18] To perform X-ray studies and Raman spectroscopy experiments, a sample was sandwiched between two diamond windows, and pressure on the sample was generated by a precise movement of two pistons, provided by a pressure-regulated flow of nitrogen gas. The smooth motion of the pistons allowed for maintenance of a constant pressure during any volume change related to phase transitions. The maximum attainable pressure was 5 kbar, and the temperature could be varied between room temperature and 300 °C.

Wide-angle X-ray powder diffraction patterns were recorded at station ID11 of the European Synchrotron Radiation Facility (ESRF) in Grenoble (France) using different wavelengths. To prevent absorption of the X-ray radiation by the diamond windows, a wavelength smaller than (or equal to) 1 Å was applied. Small-angle X-ray scattering patterns were measured at station ID2 of the same facility.

Raman spectroscopy experiments were performed with a Dilor XY-800 spectrograph coupled with a liquid nitrogen-cooled Princeton CCD array detector. The 488 nm line of a Spectra-Physics model 2012 argon laser was used as incident light, and the Raman spectra were obtained in the backscattering mode.

In addition, high-pressure DSC measurements were done with a special equipment able to measure heat flow rates at elevated pressures up to 6 kbar using silicone oil as pressure medium.[19] The high-pressure cell (the furnace), positioned in a special autoclave (Sitec, Switzerland), was connected to a commercial power-compensated DSC (Perkin-Elmer Instruments). Flat samples (5−7 mg), cut from the previously described sPS plates, were oil-tight-encapsulated in aluminum pans and heated isobarically in the HP-DSC at a heating rate of 10 or 20 K min$^{-1}$. Besides, also isothermal runs during continuous pressure rise were performed.

In the following section the consequences of the unusual density relationship in the α-phase are explored, and on the basis of the results, a $p-T$ phase diagram is proposed. It should be noted that the term phase diagram commonly refers to phases that are in thermodynamic equilibrium, but semicrystalline polymers contain only small crystals and are never in equilibrium. However, the diagrams obtained by direct plotting of the fusion data of semicrystalline polymers approach the equilibrium diagram of the crystalline material very well. Therefore, the term phase diagram will be used throughout this article, though we are aware that the results described here arise from nonequilibrium situations that are unavoidable in polymers.

The semicrystalline sample contains both an amorphous and a crystalline phase. The amorphous phase is (below $T_g$) not in an equilibrium state, and the glass process is a relaxation process rather than a phase transition. Nevertheless, the measured glass transition temperature is usually plotted in such a phase diagram as well.

## 3. Results and Discussion

**3.1. Relative Changes in the Specific Volume of the Crystalline and Amorphous Phases.** Most of the experiments have been performed with samples crystallized by heating a glassy amorphous sample above its $T_g$ (cold crystallization), implying the formation of the α-phase. Simple density measurements, using a beaker containing water and a varying amount of salt, show that the bulk density of the glass-crystallized sPS sample is lower than the density of amorphous sPS. Considering the inverse density relationship between the crystalline α-phase and the amorphous phase of sPS, this observation is in agreement with the formation of the α-phase upon crystallization from the glass.

For a semicrystalline homopolymer, in general, the difference in bulk density is proportional to the difference in electron density. Absolute differences in electron density between the crystalline and amorphous phases in a semicrystalline polymer with lamellar structure are effectively measured by small-angle X-ray scattering (SAXS). The intensity of the SAXS pattern strongly depends on the electron density fluctuation between the crystalline and amorphous region. Thus, any variation in the intensity of the SAXS pattern can be associated with specific volume changes in both regions of the semicrystalline polymer. The influence of temperature

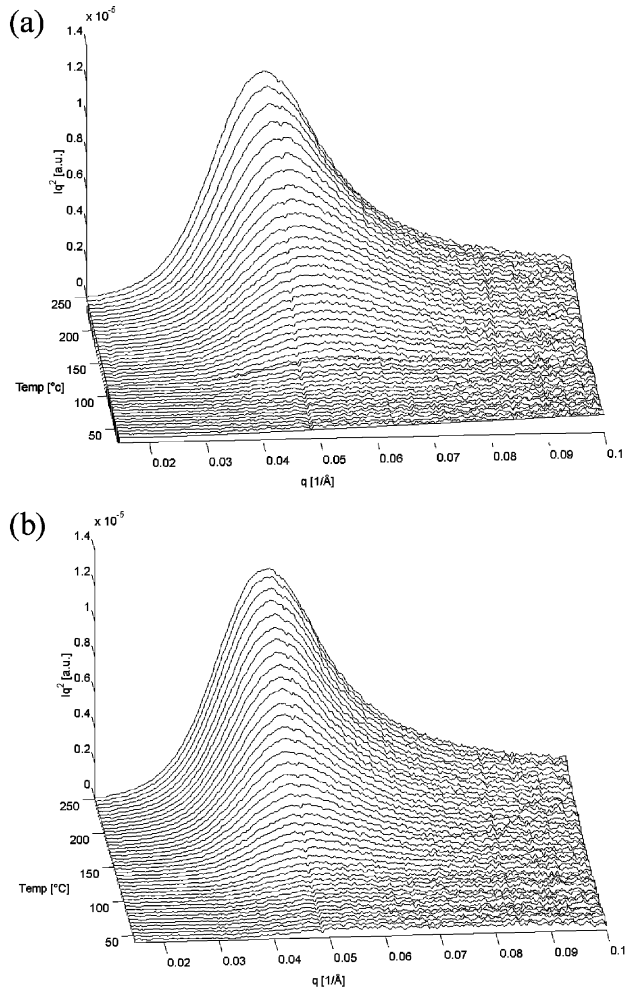


**Figure 2.** SAXS ($\lambda = 1$ Å) patterns upon (a) heating a sample in the crystalline α-phase from room temperature to 250 °C and (b) subsequent cooling.

on the SAXS data on a sample containing the α-phase is apparent from Figure 2.

At room temperature, the scattering pattern of the crystalline α-phase shows hardly any contrast. Upon heating the sample above the glass transition temperature, the intensity of the signal increases. At 250 °C, a maximum in intensity is observed around $q = 0.047$ Å$^{-1}$. This corresponds to an average long period of about 134 Å. Subsequent cooling of the sample results again in a decrease of the intensity of this maximum (while the position of the maximum stays the same), and below $T_g$ (∼100 °C) the scattering intensity is again lost.

The absence of a clear maximum intensity confirms that at room temperature the densities of the crystalline and the amorphous phase are very comparable. Generally, the thermal expansion coefficient of the amorphous phase of a semicrystalline polymer is larger than that of the crystalline phase. Consequently, the density of the amorphous phase will decrease faster than the density of the crystalline phase upon heating the sample above $T_g$. As a result, the (electron) density difference between both phases, and therefore the intensity of the maximum of the SAXS pattern, increases upon heating. The difference in thermal expansion coefficient suggests that at high temperatures ($T > T_g$) the density of the crystalline phase should be higher than that of the amorphous phase.

In view of the close density relationship between the crystalline and amorphous phases at room temperature, the density between the two phases may invert on increasing pressure, as observed earlier in P4MP1. What follows below are the SAXS/WAXD studies performed during increasing pressure at fixed temperatures above $T_g$. Figure 3 shows the SAXS data upon increasing pressure at 150, 170, and 200 °C. On the basis of the development of the SAXS pattern upon heating the sample at ambient pressure (vide supra), we anticipate that the specific volume of the amorphous phase is larger than that of the crystalline phase at the mentioned temperatures and ambient pressure. Upon increasing pressure, the SAXS intensity is lost, implying that the specific volume of both phases becomes equal. At 150 and 170 °C the loss in intensity is observed between 0.35 and 0.7 kbar, whereas at 200 °C the loss in intensity occurs between 0.7 and 1 kbar. At the corresponding pressures the WAXD pattern clearly reveals that the diffraction pattern of the crystalline α-phase remains the same. Consequently, changes in the SAXS pattern must be attributed to changes in difference in specific volume and not to loss in crystallinity. It needs to be mentioned that the loss in intensity is fully recoverable on releasing pressure again. The complete loss in intensity of the SAXS pattern refers to the existence of a $\Delta V = 0$ line in the $p-T$ diagram. The presence of a $\Delta V = 0$ line in the phase diagram suggests an inversion in $dT_m/dp$ at the point where the $\Delta V = 0$ line intersects with the melting line.

**3.2. Inversion in Clapeyron Equation.** *Wide-Angle X-ray Diffraction.* The next set of experiments was therefore to increase pressure at a constant temperature that is slightly lower than the atmospheric melting temperature. At the point where the $\Delta V = 0$ line crosses the melting line, an inversion of the melting temperature relationship is anticipated.

The WAXD data upon increasing pressure just below the atmospheric melting temperature are depicted in Figure 4. At ambient pressure, reflections distinctive for the α-phase are present (though very weak). Upon increasing pressure up to 2.4 kbar the inner reflections disappear, while at 4 kbar also the reflection arising from the phenyl rings weakens. The intensity is fully regained on releasing the pressure. It is to be noted that these experiments were performed at high temperatures (∼270 °C), close to the temperature limit of the high-pressure cell, which makes these experiments rather difficult.

*High-Pressure DSC.* Similar experiments have been performed in the HP-DSC. The pressure was raised evenly at different temperatures in the region 230−255 °C, and the heat flow rate curves were measured, respectively. Endothermic peaks were found at a certain pressure (see open circles in Figure 5), which have to be assigned to the melting of the α-phase. These results point to the existence of an inversed melting line.

To further confirm the inversed relationship, the melting temperature of the α-phase is determined by performing isobaric heating runs (see △ in Figure 5). In agreement with the isothermal DSC runs and WAXD experiments, the melting temperature of the α-phase as well as the heat of fusion decreases with increasing pressure. Besides the melting point, the isobaric heating runs also reveal the influence of pressure on the $T_g$ (open squares in Figure 5). The observed trend is similar to earlier observations by Quach and Zoller on atactic

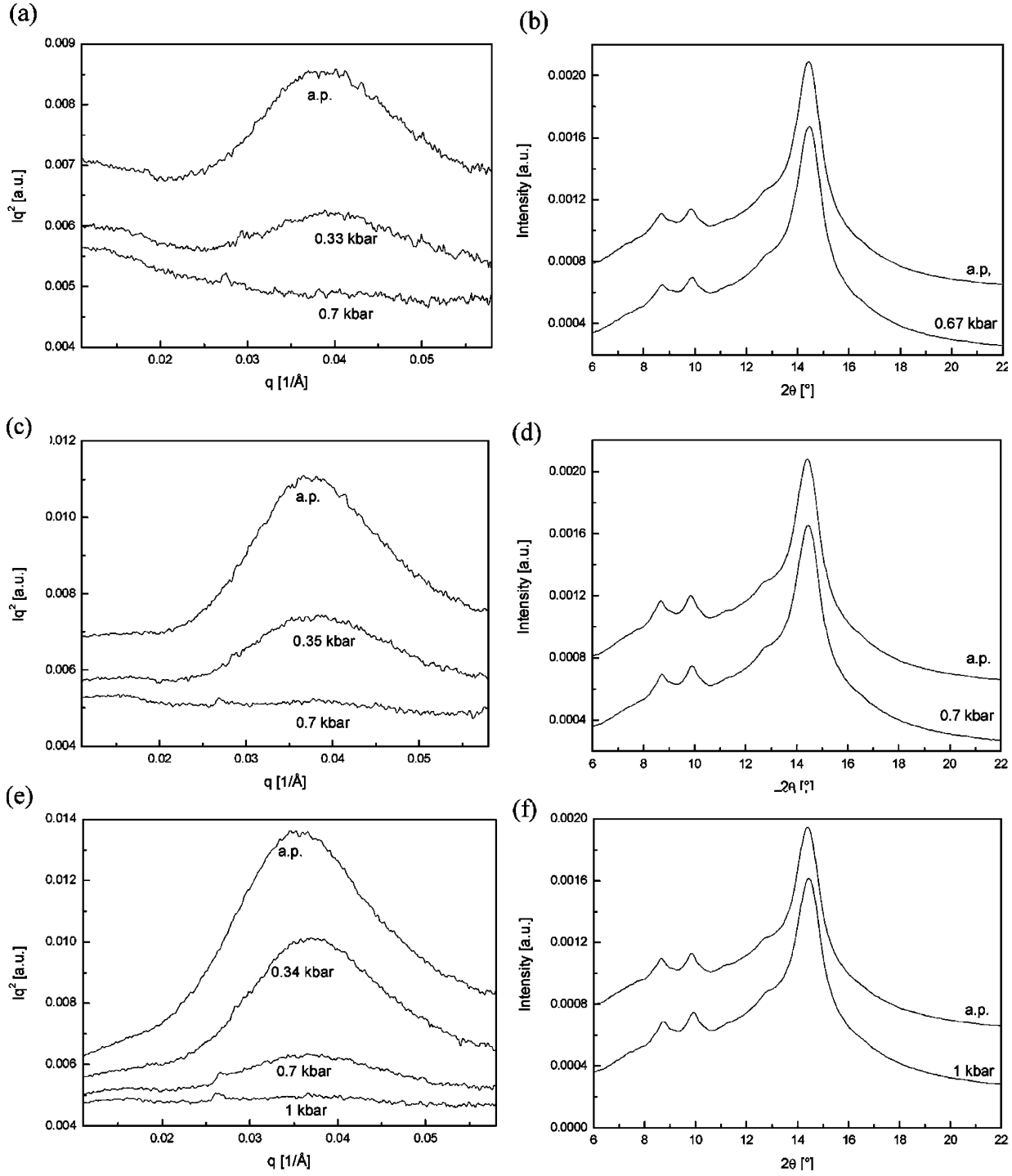


**Figure 3.** SAXS and WAXD patterns ($\lambda = 1$ Å) upon increasing pressure at fixed temperatures (above $T_g$) (a) and (b) SAXS and WAXD patterns at 150 °C, (c) and (d) SAXS and WAXD patterns at 170 °C, and (e) and (f) SAXS and WAXD patterns at 200 °C.

polystyrene, who showed that the pressure change of $T_g$ is $dT_g/dp = 30$ K kbar$^{-1}$.[20,21]

It should be notified that at isobaric pressures between 4 and 5.5 kbar no melting peaks of the α-phase could be recognized in HP-DSC, which is of relevance for the further exploration and interpretation of the phase diagram.

In addition, also the melting temperature of the most stable crystalline phase of sPS, the $\beta$-phase (as obtained by crystallization from the melt), is determined via isobaric heating runs (see ▽ in Figure 5). Unlike the α-phase, the melting temperature of the $\beta$-phase increases in this pressure region. This behavior is common for semicrystalline polymers with a dense packing of the chains.

The presence of the $\Delta V = 0$ line and the absence of melting peaks at high pressures (between 4 and 5.5 kbar) suggest the possibility of reentrant phase behavior for the α-phase of sPS. This recalls for Tamman's universal phase diagram (Figure 1). According to this phase diagram, the amorphous phase should exist at low temperatures and relatively low pressures, region III.

To validate this possibility, experiments were performed at room temperature (i.e., nearly 75 K below $T_g$) with increasing pressure.

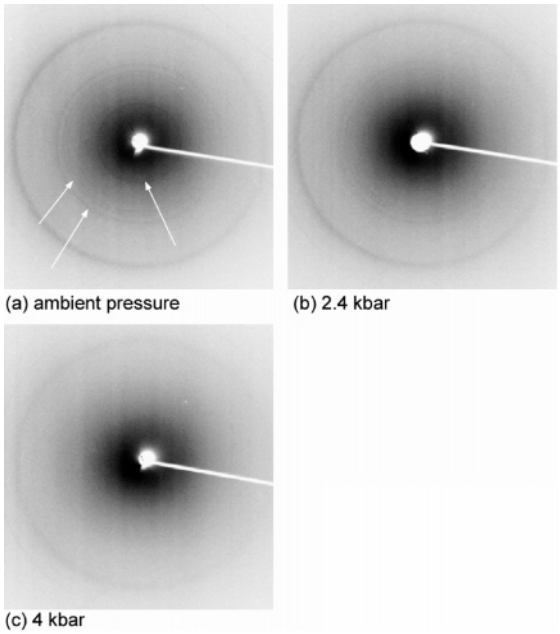


**Figure 4.** WAXS patterns ($\lambda = 1$ Å) upon increasing pressure close to the atmospheric melting temperature for the crystalline α-phase: (a) ambient pressure, (b) 2.4 kbar, (c) 4.2 kbar. Arrows indicate reflections of the α-phase.

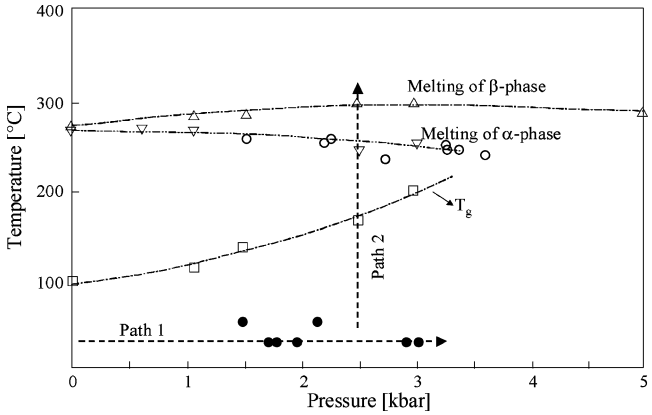


**Figure 5.** Transitions of the crystalline α- and $\beta$-phase at different pressures as measured with HP-DSC Circles in the figure represent transitions at isothermal pressure rise (like path 1); triangles represent melting points at isobaric heating (like path 2); squares show the glass transition at isobaric heating. The filled circles mark exothermic events, whereas the other transitions are all endothermic in nature. The curves are drawn to provide a guide for the eye.

**3.3. Solid-State Amorphization.** *Wide-Angle X-ray Diffraction.* The WAXD patterns upon increasing pressure at room temperature are depicted in Figure 6. As apparent, the reflections, corresponding to the crystalline α-phase, broaden and become diffuse upon increasing pressure. The reflections at relatively low diffraction angles ($2\theta = 2-8°$) disappear around 2 kbar, while a further increase of pressure results in an additional broadening of the reflection at $2\theta = 9.5°$, which is arising from the packing of the phenyl groups. The disappearance of the reflections indicates that the three-dimensional crystalline order is lost, resulting in a disordered state.

*Raman Spectroscopy.* To follow conformational changes upon increasing pressure at room temperature, Raman spectroscopy was performed, and the corresponding spectra are depicted in Figure 7. In the crystalline α-phase the backbone of the polymer adopts an all-trans

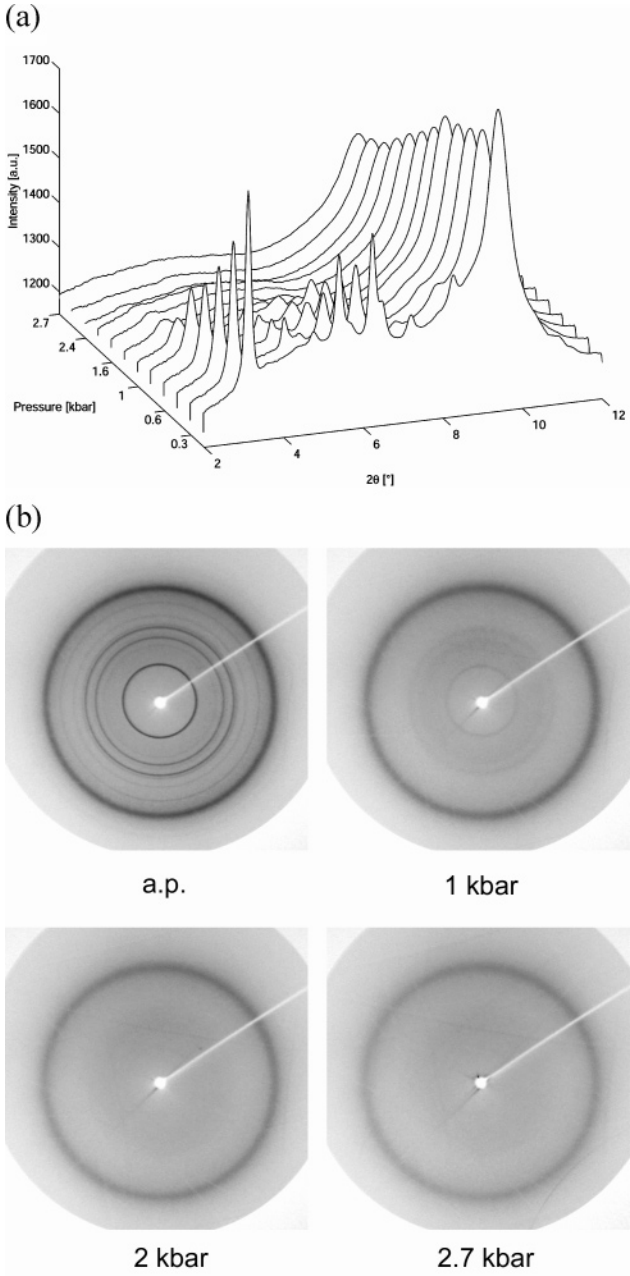


**Figure 6.** WAXD patterns ($\lambda = 0.718$ Å) upon increasing pressure at room temperature for the crystalline α-phase: (a) 3-D representation, (b) 2-D images.

planar zigzag modification, which is in the Raman spectrum characterized by a peak at 770 $cm^{-1}$. The broadening of this peak above 1.5 kbar and its complete disappearance in terms of sharpness at higher pressures imply that the all-trans planar zigzag conformation of the backbone are lost to a great extent.

Together with the nonexistence of a sharp peak at 770 $cm^{-1}$, the peak at 798 $cm^{-1}$, which is attributed to a mixture of trans and gauche conformations, spreads asymmetrically to the lower frequency region. This suggests the presence of conformational defects along the chains, which are not similar to the trans/gauche conformations obtained from the melt. The spreading to the lower frequency region can be explained as a consequence of restricted mobility that crystals will encounter upon amorphization below the glass transition temperature compared to the melting process above

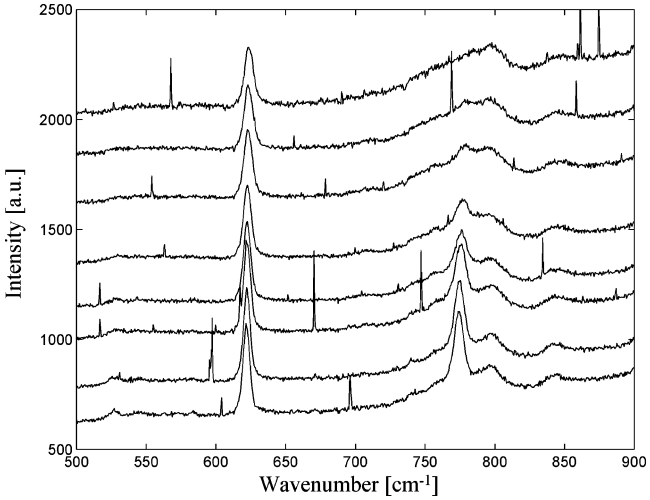


**Figure 7.** Raman spectra upon increasing pressure at room temperature for the crystalline α-phase.

the glass transition temperature. It is to be noted that, except changes in the region between 700 and 850 $cm^{-1}$, peaks only slightly broaden with pressure.

*Differential Scanning Calorimetry.* To describe possible heat effects involved in the disordering process, HP-DSC experiments were performed as well. As indicated in the phase diagram (Figure 5), the isothermal DSC run, with increasing pressure at 30 °C, results in two (very weak, well below 1 J $g^{-1}$) exothermic signals, which are observed at approximately 2 and 3 kbar, respectively. The release of heat suggests that the entropy of the sample decreases during the transformation from crystal to disordered state, thus suggesting that the entropy of the crystal is higher than its disordered state.

Some of the salient findings described in this section will be summarized; The loss in crystalline reflections in the WAXD pattern (Figure 6) occurs at a similar pressure as the disappearance of the peak at 770 $cm^{-1}$ in the Raman spectrum (Figure 7). The combination of WAXD and Raman spectroscopy suggests that upon increasing pressure conformational disordering of the crystalline lattice occurs. Furthermore, WAXD experiments suggest that the crystal to disordered state is a two-step process consisting of disordering of the main chains (∼1.5−2 kbar), followed by a disturbance of the packing of the phenyl groups (∼3 kbar). HP-DSC experiments confirm this hypothesis by the presence of the two very weak exotherms visible at mentioned pressures. The observed exotherms suggest that the entropy of the crystal is higher than its disordered state. This at first instance may seem to violate the third law of thermodynamics. Taking into consideration the reentrant nature of the phase diagram, such a unique possibility where the entropy of the crystal would be greater than that of the disordered phase would arise, as has been discussed in detail for P4MP1 elsewhere.[12]

Since the experiment is performed below $T_g$, the disordering will result in a nonequilibrium glassy state, where some structural order in the disordered state can be anticipated.[22]

What follows is a comparison between the disordered phase obtained by solid-state amorphization and via the quenched melt state. Figure 8 shows a comparison between the amorphous phase obtained via quenching from the melt (Figure 8a) and the sample as obtained upon releasing pressure after solid-state amorphization

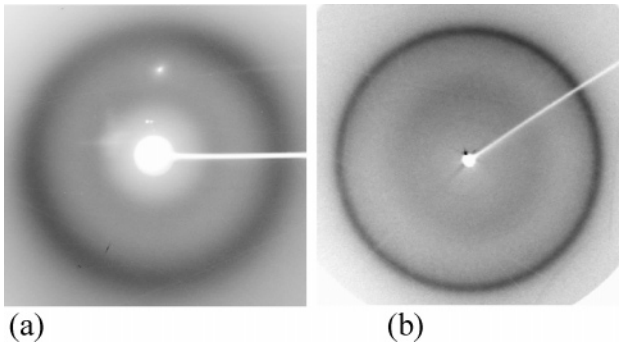


**Figure 8.** WAXD patterns at atmospheric pressure and room temperature: (a) amorphous sPS obtained on quenching from the melt; (b) sample as obtained upon releasing pressure after solid-state amorphization (see Figure 6b) of the crystalline α-phase.

(Figure 8b). A comparison of Figure 8b with Figure 6b (2.7 kbar) shows that upon releasing pressure the reflection from the phenyl ring intensifies, whereas the crystalline interchain reflections do not recover in intensity. These observations are different from the earlier reported work on P4MP1, where recovery of the crystalline reflections on releasing pressure at room temperature occurs. A possible explanation for this distinction is the larger difference between the temperature of the solid-state amorphization (RT) and the $T_g$ for sPS (∼80 °C) compared to P4MP1 (∼10 °C). This larger temperature difference hinders the crystallization process.

By comparing the diffraction pattern amorphous sPS obtained after solid-state amorphization (Figure 8b) to that of amorphous sPS obtained via quenching from the melt (Figure 8a), it can be concluded that for the former this reflection is sharper than for amorphous sPS. From here it can be concluded that though the conformational order of the polymer backbone is disturbed, the packing of the side groups is partially maintained. These observations suggest that some conformational order is retained in the glass, obtained from compression of the α-phase, suggesting the existence of a mesomorphic phase of glass as proposed by Wunderlich.[22]

The observation of disordering with the application of pressure for the crystalline α-phase is similar to the results on P4MP1 and form III of sPPMS. In combination with the results obtained upon increasing pressure close to the melting temperature (inversion in Clapeyron equation), this points to the existence of a reentrant phase behavior.

**3.4. Disordering on Cooling.** The experiments performed along two different pathways show that, below $T_g$ as well as close to the ambient melting temperature, a crystal to disorder transition occurs with the application of pressure. From a thermodynamic point of view, the disordering process that occurs at ambient temperature (below $T_g$) can be related to crossing of the melting line. The situation can either be similar to ice and silicates, for which the disordering is related to passing of the extrapolated inverse melting line[11,24,25] or to P4MP1, for which the disordering is explained by a reentry of the melt phase as predicted by Tamman and Vogel (region III, Figure 1).[11,16,26]

From the data presented in the two preceding sections it is clear that the order−disorder transition below $T_g$ takes place at low pressure. This result suggests that the transition which occurs upon increasing pressure below $T_g$ cannot be explained by simple extrapolation

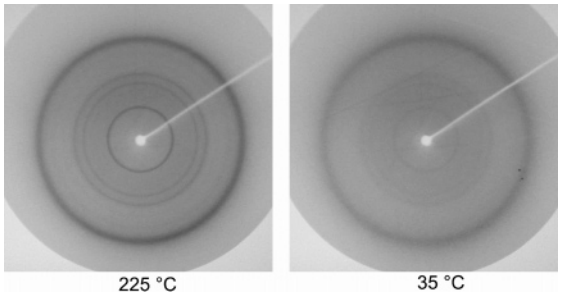


**Figure 9.** WAXD patterns at 2 kbar at 225 and 35 °C (obtained upon cooling) of the crystalline α-phase.

of the inverse melting line, like is the case for ice and silicates. It is suggested that the disordering below $T_g$ might be related to a reentry of the melt phase as predicted by Tamman. The presence of a reentrant melt phase is indicative for the possibility of inverse melting. Unlike the common situation, where melting occurs upon heating, melting should be observed upon cooling. To verify the possibility of inverse melting, an isobaric cooling experiment was performed at 2 kbar. The WAXD data upon cooling the sample from 225 °C to room temperature are depicted in Figure 9. Although the reflections not completely disappear, the broadening of the reflections and its loss in intensity imply that the sample approaches a disordered state. Despite the incomplete disordering, this result confirms the presence of a reentrant melt phase.

**3.5. Reentrant Phase Behavior.** To evaluate further the possibility of a reentrant phase behavior, experiments similar to that at room temperature have been performed at higher temperatures. Figure 10 depicts the WAXD patterns upon increasing pressure at 150, 170, and 200 °C. From these figures it follows that with the application of pressure the inner reflections slowly disappear, while at slightly higher pressures also the reflection arising from the packing of the phenyl rings ($2\theta = 14.4°$) broadens. By comparing the diffraction patterns at the different temperatures, it can be concluded that pressure at which the disordering process occurs increases with increasing temperature: at 150 °C the inner reflections disappear above 2.5 kbar, at 170 °C this occurs at 3.2 kbar, and at 200 °C (partial) disappearance of the inner reflections is observed around 3.6 kbar. This incremental correlation between temperature suggests a behavior like in region III of the Tamann diagram (Figure 1), and pressure confirms the presence of a reentrant phase behavior.

**3.6. Phase Diagram.** The combined WAXD, HP-DSC, and Raman spectroscopy experiments result in a schematic $p-T$ phase diagram for the planar zigzag modifications as depicted in Figure 11. The $\beta$-phase, for which the crystalline density at ambient pressure and temperature is higher than the amorphous density, shows the common behavior of rising $T_m$ with increasing pressure. However, the α-phase shows a much more complicated behavior due to the unusual density relationship of this phase. Two characteristic phenomena can be deduced from this phase behavior. The first is the presence of a $\Delta V = 0$ line, resulting in an inversion of the $dT_m/dp$ relationship. Second, a reentrant phase behavior is observed. To show the possible trend of the reentrant behavior, the onset of disordering (loss in packing of main chains) is presented in Figure 11 (open circles). A dotted line is drawn as a guide for the eye. It can be observed that (at least at relatively high temperatures) the reentrant $dT_m/dp$ slope has a similar course as the $dT_g/dp$ curve.

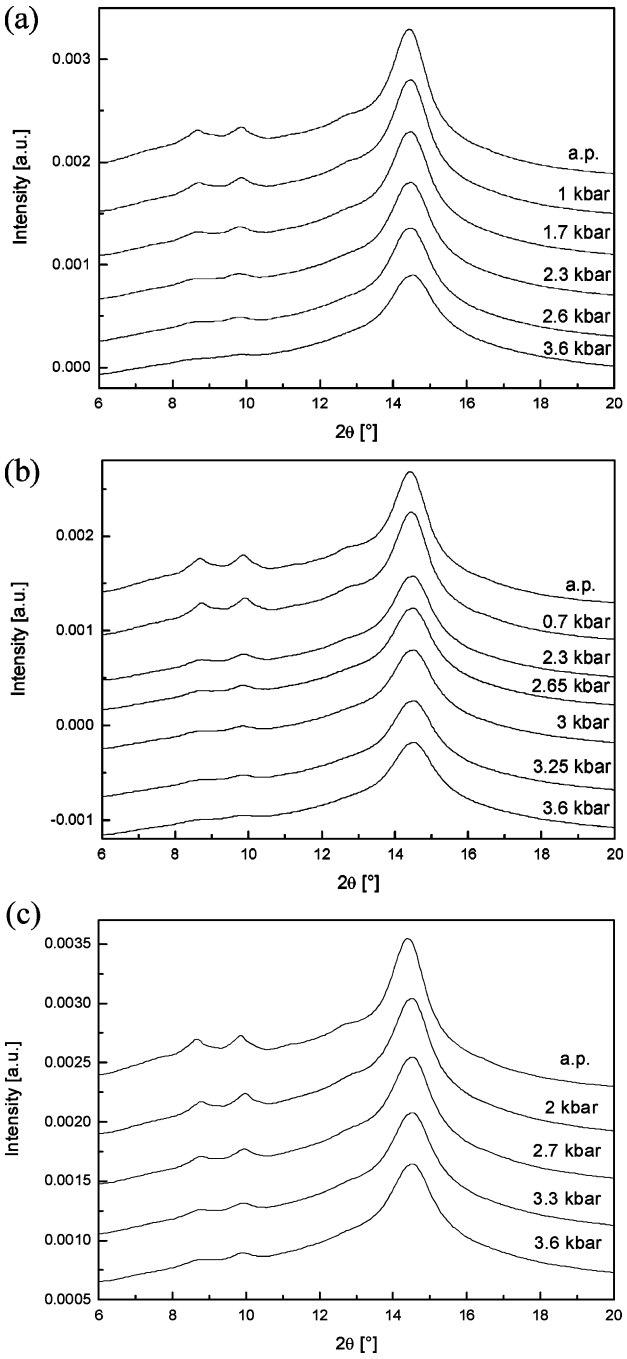


**Figure 10.** WAXD patterns upon increasing pressure at fixed temperatures ($\lambda = 1$ Å): (a) 150, (b) 170, and (c) 200 °C.

To further strengthen the argument on a reentrant phase behavior, we will recall our experimental findings on HP-DSC. The measured heat of fusion of the α-phase decreases with increasing pressure. Moreover, disordering with increasing pressure at room temperature (within region III of the phase diagram) is exothermic in nature whereas disordering close to the melting point (in region I of the phase diagram) is endothermic. These findings show that the transition from crystal to amorphous phase changes its nature from exothermic to endothermic, as one moves from region I to region III, in the $p-T$ phase diagram. This suggests the existence of a $\Delta H = 0$ line and the presence of region III in the phase diagram, as shown in Figure 1. Disordering on

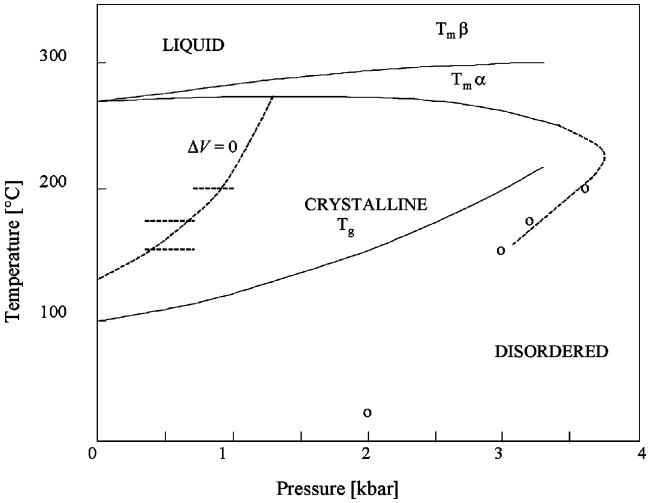


**Figure 11.** Schematic $p-T$ diagram for the planar zigzag modifications of sPS based on the results along three different pathways: solid line, $T_m$ and $T_g$ based on HP-DSC experiments; dashed line, $\Delta V = 0$ based on WAXD experiments; dashed line, possible trend of reentrant behavior based on WAXD experiments (open circles indicate onset of the melting process).

cooling further supports the existence of an amorphous region (region III) in the $p-T$ phase diagram.

As mentioned earlier in this article, no transition is observed on heating a sample from region III to region II above 3.5 kbar in the $p-T$ phase diagram, which can be explained due to the absence of crystals.

## 4. Conclusions

The loose packing of chains in the crystalline α-phase results in an unusual density relationship ($\rho_c < \rho_a$), which gives rise to a remarkable phase behavior, comparable to that of P4MP1:

(i) It has been shown that there exists a line for which the specific volume of the liquid is equal to that of the solid phase ($\Delta V = 0$ line). At the point where this line intersects with the melting line, an inversion of the sign of $dT_m/dp$ is observed.

(ii) The application of pressure at room temperature results in a disordered state. The disordering process as revealed by WAXD and Raman spectroscopy occurs at a similar pressure as melting of the crystalline α-phase as observed with HP-DSC. The disordering process takes place at much lower pressures than would be obtained upon extrapolation of the inversed melting line.

(iii) Disordering on cooling of the crystalline α-phase is observed at 2 kbar.

(iv) These observations together with differences in nature of melting (exothermic or endothermic) point to the existence of a reentrant phase behavior, as first described by Tamman in 1903.

(v) Further insight into the reentrant behavior has been obtained from experiments of increasing pressure at a fixed temperature within region III. The increase of pressure at which disordering occurs with increasing temperature confirms the possibility of a reentrant phase behavior.

## References and Notes

(1) Ishihara, N.; Seimiya, T.; Kuramoto, M.; Uoi, M. *Macromolecules* **1986**, *19*, 2464−2465.
(2) Guerra, G.; Vitagliano, V. M.; De Rosa, C.; Petraccone, V.; Corradini, P. *Macromolecules* **1990**, *23*, 1539−1544.
(3) Corradini, P.; Guerra, G. *Adv. Polym. Sci.* **1992**, *100*, 183−217.
(4) Chatani, Y.; Shimane, Y.; Inoue, Y.; Inagaki, T.; Ishioka, T. *Polymer* **1992**, *33*, 488−492.
(5) Chatani, Y.; Shimane, Y.; Ijitsu, T.; Yukinari, T. *Polymer* **1993**, *34*, 1625−1629.
(6) De Rosa, C.; Rapacciuolo, M.; Guerra, G.; Petraccone, V.; Corradini, P. *Polymer* **1992**, *33*, 1423−1428.
(7) Greis, O.; Xu, Y.; Asano, T.; Petermann, J. *Polymer* **1989**, *30*, 590−594.
(8) De Rosa, C.; Guerra, G.; Petraccone, V.; Pirozzi, B. *Macromolecules* **1997**, *30*, 4147−4152.
(9) Barnes, J. D.; McKennia, G. B.; Landes, B. G.; Bubeck, R. A.; Bank, D. *Polym. Eng. Sci.* **1997**, *37*, 1480−1484.
(10) Rastogi, S.; Newman, M.; Keller, A. *Nature (London)* **1991**, *353*, 55−57.
(11) Rastogi, S.; Newman, M.; Keller, A. *J. Polym. Sci., Part B* **1993**, *31*, 125−139.
(12) Rastogi, S.; Höhne, G. W. H.; Keller, A. *Macromolecules* **1999**, *32*, 8897−8909.
(13) Höhne, G. W. H.; Rastogi, S.; Wunderlich, B. *Polymer* **2000**, *41*, 8869−8878.
(14) Greer, L. A. *Nature (London)* **2000**, *404*, 134−135.
(15) La Camera, D. PhD Thesis, University of Napels, 2000.
(16) Tamman, G. *Kristallisieren und Schmelzen*; Johann Ambrosius Barth: Leipzig, 1903.
(17) van Ruth, N. J. L.; Rastogi, S. *Macromolecules* **2004**, *37*, 8191−8194.
(18) Hikosaka, M.; Seto, T. *Jpn. J. Appl. Phys.* **1982**, *21*, L332−L334.
(19) Höhne, G. W. H. *Thermochim. Acta* **1999**, *332*, 115−123.
(20) Quach, A.; Simha, R. *J. Appl. Phys.* **1971**, *42*, 4592−4605.
(21) Zoller, P. Z.; Walsh, D. *Standard Pressure−Volume−Temperature Data for Polymers;* Technomic Publishing Co.: Lancaster, 1995.
(22) Wunderlich, B. *Macromolecular Physics*; Academic Press: New York, 1973; Vol. 1.
(23) Mitchell, G. R.; Windle, A. H. *Polymer* **1984**, *25*, 906−920.
(24) Mishima, O.; Calvert, L. D.; Whalley, E. *Nature (London)* **1984**, *310*, 393−395.
(25) Hemley, R. J.; Chen, L. C.; Mao, H. K. *Nature (London)* **1989**, *338*, 638−640.
(26) Vogel, R. *Die Heterogenen Gleichgewichte*, 2nd ed.; Akademische Verlaggsgesellschaft Geest & Partig K.-G.: Leipzig, 1959.

MA048190B